

W/Z Bremsstrahlung as the Dominant Annihilation Channel for Dark Matter, Revisited

Nicole F. Bell,¹ James B. Dent,² Ahmad J. Galea,¹ Thomas D. Jacques,¹ Lawrence M. Krauss,² and Thomas J. Weiler³

¹*School of Physics, The University of Melbourne, Victoria 3010, Australia*

²*Department of Physics and School of Earth and Space Exploration,
Arizona State University, Tempe, AZ 85287-1404, USA*

³*Department of Physics and Astronomy, Vanderbilt University, Nashville, TN 37235, USA*

We revisit the calculation of electroweak bremsstrahlung contributions to dark matter annihilation. Dark matter annihilation to leptons is necessarily accompanied by electroweak radiative corrections, in which a W or Z boson is also radiated. Significantly, while many dark matter models feature a helicity suppressed annihilation rate to fermions, bremsstrahlung process can remove this helicity suppression such that the branching ratios $\text{Br}(\ell\nu W)$, $\text{Br}(\ell^+\ell^-Z)$, and $\text{Br}(\bar{\nu}\nu Z)$ dominate over $\text{Br}(\ell^+\ell^-)$ and $\text{Br}(\bar{\nu}\nu)$. We find this is most significant in the limit where the dark matter mass is nearly degenerate with the mass of the boson which mediates the annihilation process. Electroweak bremsstrahlung has important phenomenological consequences both for the magnitude of the total dark matter annihilation cross section and for the character of the astrophysical signals for indirect detection. Given that the W and Z gauge bosons decay dominantly via hadronic channels, it is impossible to produce final state leptons without accompanying protons, antiprotons, and gamma rays.

PACS numbers: 95.35.+d, 12.15.Lk, 95.85.Ry

I. INTRODUCTION

The importance of electroweak radiative corrections to dark matter annihilation has recently been recognized, and examined in a number of publications [1–10]. In a recent paper some of the present authors considered electroweak bremsstrahlung contributions to dark matter annihilation, in models in which dark matter annihilation to a fermion-antifermion pair, $\chi\chi \rightarrow \bar{f}f$, is helicity suppressed [1]. There it was shown that W/Z bremsstrahlung lifts helicity suppressions, and can therefore be the dominant DM annihilation mode. However, the explicit cross section calculation in Ref. [1] was in error, and thus some of the quantitative conclusions of that work must be modified. The purpose of the present paper is to revisit the calculation of the W/Z bremsstrahlung cross sections, and discuss their implications. The main result is that the three body final state processes can still dominate the tree level process, but is now found to be most pronounced in the region where the parameter $\mu \equiv m_\eta^2/m_\chi^2$ is close to one, with m_η and m_χ being the mass of the boson which mediates the annihilation process and the dark matter mass, respectively. This region of parameter space is reminiscent of the co-annihilation region in standard supersymmetric (SUSY) scenarios, although the present work can also be applied to models which are not in the SUSY framework.

Let us parametrize the dark matter annihilation cross section in the usual way,

$$\sigma v = a + bv^2, \quad (1)$$

where the constant a arises from s -wave annihilation while the constant b receives contributions from both s - and p -wave channels. Since the dark matter velocity in a galactic halo today is $v \sim 10^{-3}c$, the p -wave term is

strongly velocity suppressed. In order to have a large annihilation cross section in the Universe today, it is desirable to have an unsuppressed a (s -wave) term. However, the s -wave annihilation of DM to a fermion-antifermion pair is helicity suppressed in a number of important and popular models. The most well known example is the annihilation of supersymmetric neutralinos to a fermion-antifermion pair. The circumstances under which helicity suppressions do or do not arise were discussed in detail in Ref [1], which we briefly recapitulate in Appendix A.

It has long been known that bremsstrahlung of photons can lift such a helicity suppression, leading to the result that the cross section for $\chi\chi \rightarrow \bar{f}f\gamma$ can dominate over that for $\chi\chi \rightarrow \bar{f}f$ [11–16]. However, the fact that radiation of a W or Z gauge boson would also lift a helicity suppression had been overlooked until the work of Refs. [1, 4]. In these scenarios for which the helicity suppression is removed, the dominant annihilation channels are the set of bremsstrahlung processes, namely γ , W and Z bremsstrahlung. (If the dark matter annihilates to colored fermions, radiation of gluons would also contribute). The phenomenology of W and Z bremsstrahlung is richer than that for photon bremsstrahlung alone. This is because the W and Z bosons decay dominantly to hadronic final states, including antiprotons, for which interesting cosmic ray bounds exist.

II. EXAMPLE OF SUPPRESSED ANNIHILATION

To illustrate our arguments, we choose a simple example of the class of model under discussion. This is provided by the leptophilic model proposed in Ref. [17, 18]. Here the DM consists of a gauge-singlet Majorana

fermion χ which annihilates to leptons via the $SU(2)$ -invariant interaction term

$$f(\nu\ell^-)_L \varepsilon \begin{pmatrix} \eta^+ \\ \eta^0 \end{pmatrix} \chi + h.c. = f(\nu_L\eta^0 - \ell_L^-\eta^+)\chi + h.c. \quad (2)$$

where f is a coupling constant, ε is the 2×2 antisymmetric matrix, and (η^+, η^0) is a new $SU(2)$ doublet scalar. In this model, DM annihilation to fermions is mediated by t and u channel exchange of the η fields.

An identical coupling occurs in supersymmetry if we identify χ with a neutralino and η with a sfermion doublet. In fact, the implementation of supersymmetric photinos as dark matter by H. Goldberg provided the first explicit calculation of s -wave suppressed Majorana dark matter annihilation to a fermion pair [19]. Therefore, much of what we discuss below is also relevant for neutralino annihilation to fermions via the exchange of sfermions. However, the class of models for which the $2 \rightarrow 2$ annihilation is helicity suppressed is more general than the class of supersymmetric models.

The cross section for the $2 \rightarrow 2$ process $\chi\chi \rightarrow e^+e^-$ or $\nu\bar{\nu}$ is given by

$$v\sigma = \frac{f^4 v^2}{24\pi m_\chi^2} \frac{1 + \mu^2}{(1 + \mu)^4}, \quad (3)$$

where $m_l \simeq 0$ and $m_{\eta^\pm} = m_{\eta^0}$ have been assumed, and $\mu = m_\eta^2/m_\chi^2$. The suppressions discussed above are apparent in Eq. (3). The helicity suppressed s -wave term is absent in the $m_l = 0$ limit, and thus only the v^2 -suppressed term remains.

III. LIFTING THE SUPPRESSION WITH ELECTROWEAK BREMSSTRAHLUNG

A. W-strahlung cross section

We shall take the limit $m_l \simeq 0$ and assume that $m_{\eta^\pm} = m_{\eta^0}$. The matrix elements for the six diagrams of Fig. 1 are given by

$$\mathcal{M}_a = i \frac{f^2 g}{\sqrt{2}} \frac{1}{q_1^2} \frac{1}{t_1 - m_\eta^2} \times (\bar{v}(k_2) P_L v(p_2)) (\bar{u}(p_1) \gamma^\mu P_L \not{q}_1 u(k_1)) \epsilon_\mu^Q, \quad (4)$$

$$\mathcal{M}_b = i \frac{f^2 g}{\sqrt{2}} \frac{1}{q_1^2} \frac{1}{u_1 - m_\eta^2} \times (\bar{v}(k_1) P_L v(p_2)) (\bar{u}(p_1) \gamma^\mu P_L \not{q}_1 u(k_2)) \epsilon_\mu^Q, \quad (5)$$

$$\mathcal{M}_c = -i \frac{f^2 g}{\sqrt{2}} \frac{1}{q_2^2} \frac{1}{t_2 - m_\eta^2} \times (\bar{v}(k_2) P_L \not{q}_2 \gamma^\mu v(p_2)) (\bar{u}(p_1) P_R u(k_1)) \epsilon_\mu^Q, \quad (6)$$

$$\mathcal{M}_d = -i \frac{f^2 g}{\sqrt{2}} \frac{1}{q_2^2} \frac{1}{u_2 - m_\eta^2} \times ((\bar{v}(k_1) P_L \not{q}_2 \gamma^\mu v(p_2)) (\bar{u}(p_1) P_R u(k_2)) \epsilon_\mu^Q), \quad (7)$$

$$\mathcal{M}_e = -i \frac{f^2 g}{\sqrt{2}} \frac{1}{t_3 - m_\eta^2} \frac{1}{t'_3 - m_\eta^2} \times ((\bar{v}(k_2) P_L v(p_2)) (\bar{u}(p_1) P_R u(k_1)) \times ((k_1 - p_1) + (k_1 - p_1 - Q))^\mu \epsilon_\mu^Q), \quad (8)$$

$$\mathcal{M}_f = -i \frac{f^2 g}{\sqrt{2}} \frac{1}{u_3 - m_\eta^2} \frac{1}{u'_3 - m_\eta^2} \times ((\bar{v}(k_1) P_L v(p_2)) (\bar{u}(p_1) P_R u(k_2)) \times ((k_2 - p_1) + (k_2 - p_1 - Q))^\mu \epsilon_\mu^Q), \quad (9)$$

where we define the usual helicity projectors $P_{R/L} \equiv \frac{1}{2}(1 \pm \gamma_5)$, and the Mandelstam variables

$$\begin{aligned} t_1 &= (k_1 - q_1)^2, \\ t_2 &= (k_1 - p_1)^2, \\ u_1 &= (k_2 - q_1)^2, \\ u_2 &= (k_2 - p_1)^2, \\ t_3 &= (k_1 - p_1)^2 = t_2, \\ t'_3 &= (k_2 - p_2)^2 = (k_1 - p_1 - Q)^2, \\ u_3 &= (k_2 - p_1)^2 = u_2, \\ u'_3 &= (k_1 - p_2)^2 = (k_2 - p_1 - Q)^2. \end{aligned} \quad (10)$$

The vertex factors used in the matrix elements are as follows: the νW vertex has an $\frac{ig}{\sqrt{2}} \gamma^\mu P_L \epsilon_\mu^Q$, the $\chi\eta l$ vertex is ifP_L , and the coupling between the W^- and the $\eta^+ - \eta^0$ is taken to be of the form $-ig(p + p')/\sqrt{2}$ from Ref. [20]. Fierz transformed versions of these matrix elements, and some insight gained from them, are collected in Appendix C.

We have explicitly checked the gauge invariance of our set of Feynman diagrams. Writing the matrix element as

$$\mathcal{M} = \mathcal{M}^\mu \epsilon_\mu^Q, \quad (11)$$

the Ward identity

$$Q_\mu \mathcal{M}^\mu = 0, \quad (12)$$

is satisfied for the sum of the diagrams. The Ward identity takes the same form as for photon bremsstrahlung provided we take the lepton masses to be zero, since the axial vector current is conserved in this limit. Note that diagrams (a)+(c)+(e) form a gauge invariant subset, as do (b)+(d)+(f). The full amplitude is the sum of the partial amplitudes, properly weighted by a minus sign when two fermions are interchanged. Thus we have $\mathcal{M} = (\mathcal{M}_a + \mathcal{M}_c + \mathcal{M}_e) - (\mathcal{M}_b + \mathcal{M}_d + \mathcal{M}_f)$.

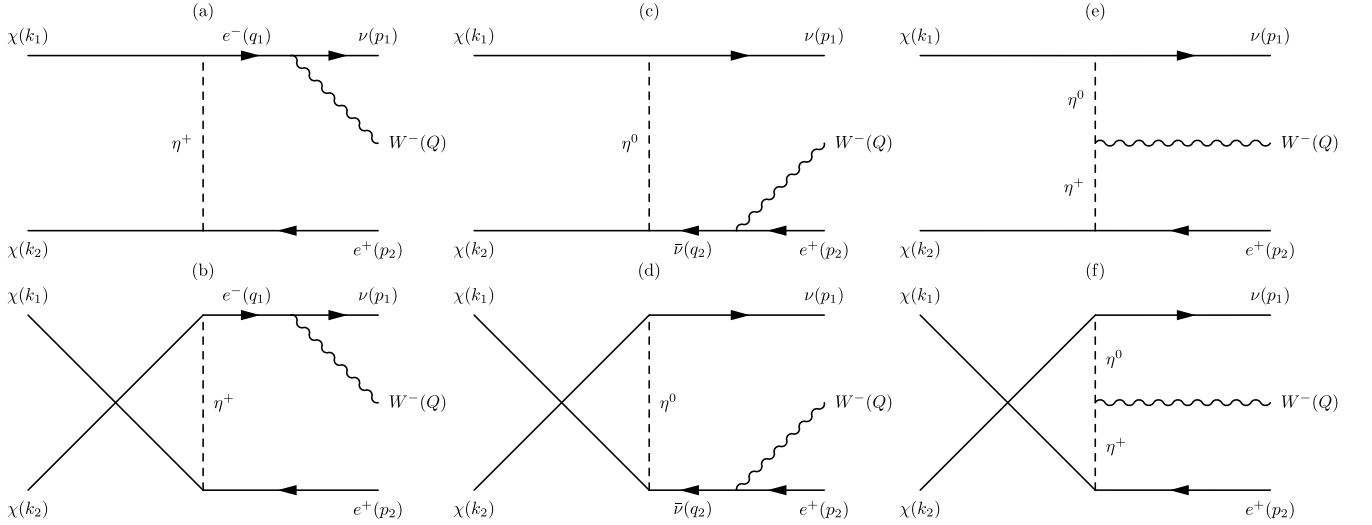


FIG. 1. The t -channel ((a),(c), and (e)) and u -channel ((b), (d) and (f)) Feynman diagrams for $\chi\chi \rightarrow e^+\nu W^-$. Note that t - and u -channel amplitudes are simply related by the $k_1 \leftrightarrow k_2$ interchange symmetry. All fermion momenta in the diagrams flow with the arrow except p_2 and q_2 , with $q_1 = p_1 + Q$, $q_2 = p_2 + Q$.

In performing the sum over spins and polarizations, we note the standard polarization sum,

$$\sum_{\text{pol.}} \epsilon_\mu^Q \epsilon_\nu^Q = - \left(g_{\mu\nu} - \frac{Q_\mu Q_\nu}{m_W^2} \right), \quad (13)$$

can be replaced with $-g_{\mu\nu}$ alone. The Ward identity of Eq.(12) ensures the second term in Eq.(13) does not contribute once the contributions from all diagrams are summed (and squared).

In addition, we find that the longitudinal polarization of the W also does not contribute to the s -wave amplitude, i.e.

$$\mathcal{M}^\mu \epsilon_{L\mu}^Q = 0. \quad (14)$$

The W boson behaves as a massive transverse photon, with just two transverse polarizations contributing. As a consequence, our calculation of W bremsstrahlung must reduce to the known results for photon bremsstrahlung in the $m_W \rightarrow 0$ limit, modulo coupling constants. Below we will show that this happens.

The thermally-averaged cross section is given by

$$v d\sigma = \frac{1}{2s} \int \frac{1}{4} \sum_{\text{spin, pol.}} |\mathcal{M}|^2 dLips^3 \quad (15)$$

where the $\frac{1}{4}$ arises from averaging over the spins of the initial χ pair, $v = \sqrt{1 - \frac{4m_\chi^2}{s}}$ is the mean dark matter velocity, as well as the dark matter single-particle velocity in the center of mass frame¹, and $dLips^n$ represents n -body Lorentz invariant phase space.

The three-body Lorentz Invariant Phase Space is

$$dLips^3 = (2\pi)^4 \frac{d^3\vec{p}_1}{2E_1} \frac{d^3\vec{p}_2}{2E_2} \frac{d^3\vec{Q}}{2E_W} \frac{\delta^4(P - p_1 - p_2 - Q)}{(2\pi)^9} \quad (16)$$

where $P = k_1 + k_2$. This factorizes into the product of two two-body phase space integrals, convolved with an integral over the fermion propagator momentum,

$$\begin{aligned} dLips^3 &= \int_{m_W^2}^s \frac{dq_1^2}{2\pi} \left(\frac{d^3\vec{q}_1}{2E_{q_1}} \frac{d^3\vec{p}_2}{2E_2} \frac{\delta^4(P - q_1 - p_2)}{(2\pi)^2} \right) \\ &\times \left(\frac{d^3\vec{p}_1}{2E_1} \frac{d^3\vec{Q}}{2E_W} \frac{\delta^4(q_1 - Q - p_1)}{(2\pi)^2} \right) \\ &= \int_{m_W^2}^s \frac{dq_1^2}{2\pi} dLips^2(P^2, q_1^2, p_2^2) dLips^2(q_1^2, Q^2, p_1^2). \end{aligned} \quad (17)$$

Evaluating the two-body phase space factors in their respective center of momentum frames, and using $p_1^2 = p_2^2 = 0$, we have

$$dLips^2(x^2, y^2, 0) = \frac{x^2 - y^2}{8\pi x^2} \frac{d\Omega}{4\pi}. \quad (18)$$

This allow us to write the three-body phase space as

$$\begin{aligned} dLips^3 &= \frac{1}{2^6 (2\pi)^4} \int_{M_W^2}^s dq_1^2 \\ &\times \frac{(s - q_1^2)(q_1^2 - Q^2)}{s q_1^2} d\phi d \cos \theta_P d \cos \theta_q, \end{aligned} \quad (19)$$

where ϕ is the angle of intersection of the plane defined by $\chi\chi \rightarrow ee^*$ with that defined by $e\nu W$, and θ_P and θ_q are defined in the P (CoM) and q rest frames respectively.

We calculate the cross section for W emission following the procedure outlined above and expand in powers of the DM velocity, v , keeping only the leading order (v^0) contribution. As expected, we have an unsuppressed cross section given by

$$\begin{aligned}
\sigma v \simeq \frac{\alpha_W f^4}{256\pi^2 m_\chi^2} \left\{ (\mu + 1) \left[\frac{\pi^2}{6} - \ln^2 \left(\frac{2m_\chi^2(\mu + 1)}{4m_\chi^2\mu - m_W^2} \right) - 2\text{Li}_2 \left(\frac{2m_\chi^2(\mu + 1) - m_W^2}{4m_\chi^2\mu - m_W^2} \right) \right. \right. \\
+ 2\text{Li}_2 \left(\frac{m_W^2}{2m_\chi^2(\mu + 1)} \right) - \text{Li}_2 \left(\frac{m_W^2}{m_\chi^2(\mu + 1)^2} \right) - 2\text{Li}_2 \left(\frac{m_W^2(\mu - 1)}{2(m_\chi^2(\mu + 1)^2 - m_W^2)} \right) \\
+ 2 \ln \left(\frac{4m_\chi^2\mu - m_W^2}{2m_\chi^2(\mu - 1)} \right) \ln \left(1 - \frac{m_W^2}{2m_\chi^2(\mu + 1)} \right) + \ln \left(\frac{m_W^2(\mu - 1)^2}{4(m_\chi^2(\mu + 1)^2 - m_W^2)} \right) \ln \left(1 - \frac{m_W^2}{m_\chi^2(\mu + 1)^2} \right) \left. \right] \\
+ \frac{(4\mu + 3)}{(\mu + 1)} - \frac{m_W^2(4m_\chi^2(\mu + 1)(4\mu + 3) - (m_W^2 - 4m_\chi^2)(\mu - 3))}{16m_\chi^4(\mu + 1)^2} \\
+ \frac{m_W^2(4m_\chi^4(\mu + 1)^4 - 2m_W^2m_\chi^2(\mu + 1)(\mu + 3) - m_W^4(\mu - 1))}{4m_\chi^4(\mu + 1)^3(m_\chi^2(\mu + 1)^2 - m_W^2)} \ln \left(\frac{m_W^2}{4m_\chi^2} \right) \\
+ \ln \left(\frac{2m_\chi^2(\mu - 1)}{2m_\chi^2(\mu + 1) - m_W^2} \right) \frac{(\mu - 1)(2m_\chi^2(\mu + 1) - m_W^2)}{4m_\chi^4(\mu + 1)^3(4m_\chi^2\mu - m_W^2)(m_\chi^2(\mu + 1)^2 - m_W^2)} \\
\left. \times (4m_\chi^6(\mu + 1)^4(4\mu + 1) - m_\chi^4m_W^2(\mu + 1)^2(3\mu(\mu + 6) + 7) + 2m_\chi^2m_W^4(\mu(\mu + 4) + 1) - m_W^6) \right\} \quad (20)
\end{aligned}$$

where $\alpha_W \equiv g^2/(4\pi)$. The Spence function (or “dilogarithm”) is defined as $\text{Li}_2(z) \equiv -\int_0^z \frac{d\zeta}{\zeta} \ln|1 - \zeta| = \sum_{k=1}^{\infty} \frac{z^k}{k^2}$.

If we take the limit $m_W \rightarrow 0$ and replace α_W with $2\alpha_{\text{em}}$, then Eq. (20) reproduces the cross section for bremsstrahlung of photons, namely²

$$\sigma v \simeq \frac{\alpha_{\text{em}} f^4}{128\pi^2 m_\chi^2} \left\{ (\mu + 1) \left[\frac{\pi^2}{6} - \ln^2 \left(\frac{\mu + 1}{2\mu} \right) - 2\text{Li}_2 \left(\frac{\mu + 1}{2\mu} \right) \right] + \frac{4\mu + 3}{\mu + 1} + \frac{4\mu^2 - 3\mu - 1}{2\mu} \ln \left(\frac{\mu - 1}{\mu + 1} \right) \right\}. \quad (21)$$

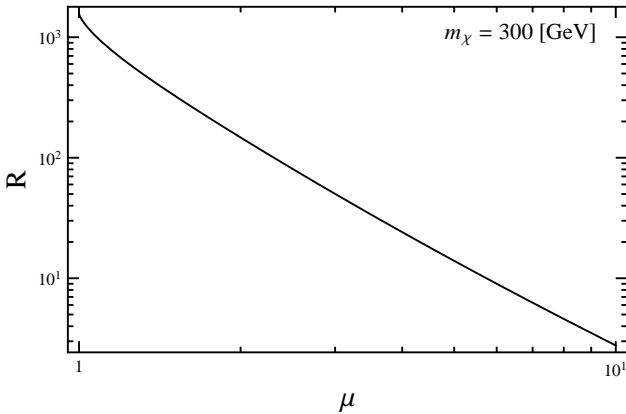


FIG. 2. The ratio $R = v\sigma(\chi\chi \rightarrow e^+\nu W^-)/v\sigma(\chi\chi \rightarrow e^+e^-)$ as a function of $\mu = (m_\eta/m_\chi)^2$, for $m_\chi = 300$ GeV. We have used $v = 10^{-3}c$, appropriate for the Galactic halo.

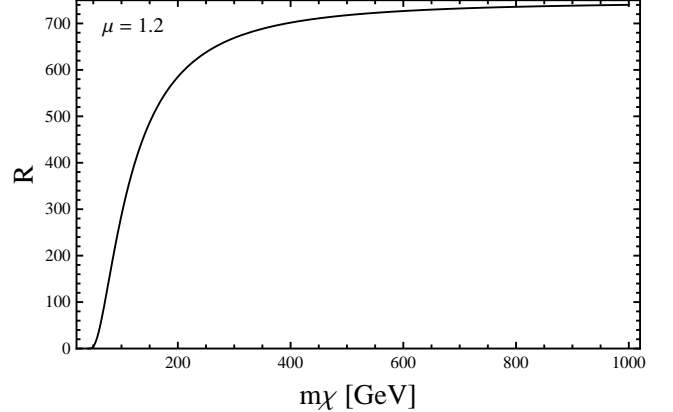


FIG. 3. The ratio $R = v\sigma(\chi\chi \rightarrow e^+\nu W^-)/v\sigma(\chi\chi \rightarrow e^+e^-)$ as a function of the DM mass m_χ , for $\mu = 1.2$ GeV. We have used $v = 10^{-3}c$, appropriate for the Galactic halo.

The successful recovery of the photon bremsstrahlung result in the massless W limit provides a check

on the rather complicated expression for massive W bremsstrahlung given above in Eq.(20).

Since we are working in the limits $v = 0$ and $m_f = 0$, the nonzero results in Eqs.(20) and (21) imply that the leading terms are neither helicity nor velocity suppressed. Not clear from the mathematical expressions is the sensible fact that the cross sections fall monotonically with increasing m_η (or μ). This monotonic fall is shown in Fig. 2, where we plot the ratio of the W -

¹ Informative discussions of the meaning of v are given in [21], and the inclusion of thermal averaging is covered in [22].

² Note that Eq.2. of Ref. [15] is larger by an overall factor of two, and also has the opposite sign for the $(1+\mu)[\dots]$ term, while Eq.1. of Ref. [15] is consistent with our results.

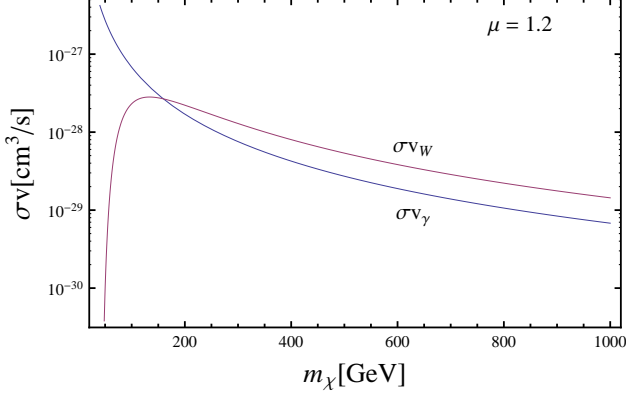


FIG. 4. The cross sections for $\chi\chi \rightarrow e^+\nu W^-$ (red) and $\chi\chi \rightarrow e^+e^-\gamma$ (blue), for $\mu = 1.2$ and coupling $f = 1$. For large DM mass, the cross sections differ by a factor of $1/(2\sin^2\theta_W) = 2.17$ while for m_χ comparable to m_W the W bremsstrahlung cross section is suppressed by phase space effects.

strahlung cross section to that of the lowest order process, $R = v\sigma(\chi\chi \rightarrow e^+\nu W^-)/v\sigma(\chi\chi \rightarrow e^+e^-)$. The lowest order process itself falls as μ^{-2} , so the W -strahlung process falls as μ^{-4} . This latter dependence is expected for processes with two propagators each off-shell by $1/\mu$, thereby signaling leading order cancellations among Fig. 1 diagrams (a)-(d).

Importantly, the effectiveness of the W -strahlung processes in lifting suppression of the annihilation rate is evident in Fig. 2. The ratio is maximized for μ close to 1, where m_χ and m_η are nearly degenerate. However, the W -strahlung process dominates over the tree level annihilation even if a mild hierarchy between m_χ and m_η is assumed. The ratio exceeds 100 for $\mu \lesssim 2$.

Fig. 3 illustrates that the ratio R is insensitive to the DM mass, except for low m_χ where the W mass significantly impacts phase space. From the figure one gleans that for $m_\chi \gtrsim 3m_W$, the ratio R is already near to its

asymptotic value. Incidentally, the asymptotic value may be obtained analytically by dividing Eq. (21) with Eq. (3) and rescaling α_{em} with $\alpha_W/2$.

In Fig. 4 we compare the W -strahlung cross section with that for photon bremsstrahlung. For high dark matter masses where the W mass is negligible, the two cross section are identical except for the overall normalization, which is higher by factor of $1/(2\sin^2\theta_W) = 2.17$ for W -strahlung. For lower DM mass, the available phase space is reduced due to W mass effects, and thus the W -strahlung cross section falls below that for photons. This can be seen in Fig. 4 for $m_\chi \lesssim 150$ GeV (this number is fairly insensitive to μ). Another factor of two is gained for W -strahlung when the W^+ mode is added to the W^- mode shown here.

Nominally, the correct dark matter energy fraction is obtained for early-Universe thermal decoupling with an annihilation cross section of $3 \times 10^{-26} \text{cm}^3/\text{s}$. It is seen in Fig. 4 that the W -strahlung mode falls 2-3 orders of magnitude below this value. Note that at the time of dark matter freeze-out in the early Universe, the velocity suppression of the p-wave contribution is not as severe as it is for late-Universe annihilation. Hence, radiative W -strahlung with its natural suppression factor $\alpha_W/4\pi$ is probably not the dominant annihilation mode responsible for early-Universe decoupling of Majorana dark matter.

B. W and Lepton Spectra

To obtain the energy spectrum of the W , we compute the differential cross section in terms of E_W by making the transformation

$$d\cos(\theta_q) \rightarrow \frac{-4\sqrt{s}q^2}{(s-q^2)(q^2-m_W^2)} dE_W. \quad (22)$$

The energy spectrum of the the primary leptons is calculated in similar fashion. We find

$$v \frac{d\sigma}{dx_W} = \frac{\alpha_W f^4}{128\pi^2 m_\chi^2} \left((1-x_W) + \frac{m_W^2}{4m_\chi^2} \right) \left\{ \sqrt{x_W^2 - \frac{m_W^2}{m_\chi^2}} \left[\frac{2}{((\mu+1)(\mu+1-2x_W) + \frac{m_W^2}{m_\chi^2})} - \frac{1}{(\mu+1-x_W)^2} \right] - \frac{((\mu+1)(\mu+1-2x_W) + \frac{m_W^2}{m_\chi^2})}{2(\mu+1-x_W)^3} \ln \left(\frac{\mu+1-x_W + \sqrt{x_W^2 - m_W^2/m_\chi^2}}{\mu+1-x_W - \sqrt{x_W^2 - m_W^2/m_\chi^2}} \right) \right\}, \quad (23)$$

$$v \frac{d\sigma}{dx_l} = \frac{\alpha_W f^4}{512\pi^2 m_\chi^2} \frac{1}{(\mu-1+2x_l)^2} \left\{ \left(4(1-x_l)^2 - 4x_l(\mu+1) + 3(\mu+1)^2 - \frac{m_W^2}{m_\chi^2}(\mu+3) \right) \times \ln \left(\frac{2m_\chi^2(\mu+1)(1-x_l) - m_W^2}{(2m_\chi^2(\mu+1-2x_l) - m_W^2)(1-x_l)} \right) - \frac{x_l(4m_\chi^2(1-x_l) - m_W^2)}{(2m_\chi^2(1-x_l)(\mu+1) - m_W^2)(1-x_l)^2} \times \left[(1-x_l)^2(4(1-x_l)^2 - x_l(\mu+1) + 3(\mu+1)^2) + \frac{m_W^2}{4m_\chi^2}(1-x_l)(x_l(\mu+11) - 4(\mu+3)) - x_l \frac{m_W^2}{8m_\chi^2} \right] \right\}. \quad (24)$$

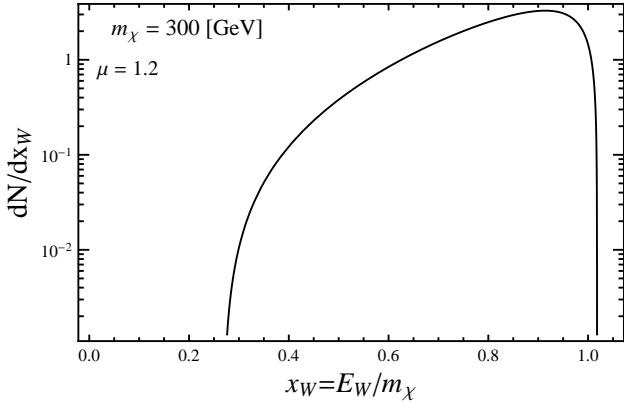


FIG. 5. The W spectrum per $\chi\chi \rightarrow e\nu W$ annihilation for $m_\chi = 300$ GeV and $\mu = 1.2$.

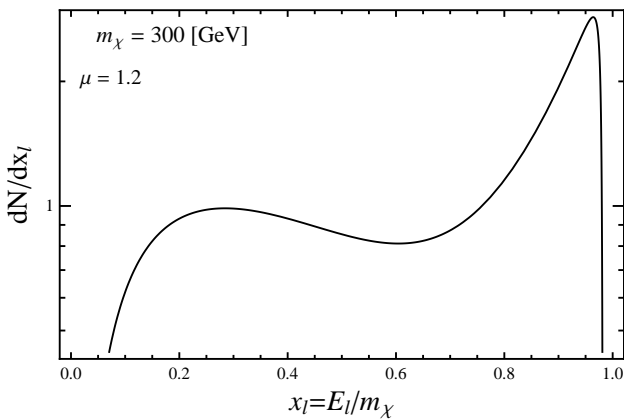


FIG. 6. The primary lepton spectrum per $\chi\chi \rightarrow e\nu W$ annihilation, for $m_\chi = 300$ GeV and $\mu = 1.2$.

The W spectrum per $\chi\chi \rightarrow e\nu W$ event is given in Fig. 5. We use the scaling variable $x_W \equiv E_W/m_\chi$, and plot $dN/dx_W \equiv (\frac{1}{\sigma_{e^+\nu W^-}}) \frac{d\sigma_{e^+\nu W^-}}{dx_W}$. The kinematic range of x_W is $[\frac{m_W}{m_\chi}, (1 + \frac{m_W^2}{4m_\chi^2})]$, with the lower limit corresponding to a W produced at rest, and the upper limit corresponding to parallel lepton momenta balancing the opposite W momentum. As evident in Fig. 5, the W boson spectrum has a broad energy distribution, including a significant high energy component.

For the lepton energy spectrum, the range of the scaling variable $x_\ell \equiv E_\ell/m_\chi$ is $[0, 1 - \frac{m_W^2}{4m_\chi^2}]$. Both limits arise when one lepton has zero energy and the other is produced back-to-back with the W . The lepton spectrum is shown in Fig. 6. Note that this spectrum is valid for either the e^+ or the ν from the annihilation $\chi\chi \rightarrow e^+\nu W^-$, and for either e^- or $\bar{\nu}$ from the annihilation $\chi\chi \rightarrow e^-\bar{\nu} W^+$.

C. Z Emission

Consider the process producing the $\bar{\nu}\nu Z$ final state. The cross sections for the Z -strahlung processes are related to those for W -strahlung in a simple way: The amplitudes producing $\bar{\nu}\nu Z$ arise from the same six graphs of Fig.1, where e , W and η^+ are replaced everywhere by ν and Z and η_0 , respectively. The calculation of the amplitudes, and their interferences, proceeds in an identical fashion. After making the replacement $m_W \rightarrow m_Z$, the cross section for the annihilation process $\chi\chi \rightarrow \nu\bar{\nu} Z$ differs from that for $\chi\chi \rightarrow e^+\nu W^-$ by only an overall normalization factor,

$$\begin{aligned} v \sigma_{\nu\bar{\nu} Z} &= \frac{1}{(2 \cos^2 \theta_W)} \times v \sigma_{e^+\nu W^-} \Big|_{m_W \rightarrow m_Z} \\ &\simeq 0.65 \times v \sigma_{e^+\nu W^-} \Big|_{m_W \rightarrow m_Z}. \end{aligned} \quad (25)$$

Consider now the $e^+e^- Z$ final state. Again, the amplitudes arise from the same six basic graphs of Fig.1. Since only the left-handed leptons couple to the dark matter via the $SU(2)$ doublet η , only the left handed component of e^- participates in the interaction with the Z . Therefore, the couplings of the charged leptons to Z and W take the same form, up to a normalization constant. We thus find

$$\begin{aligned} v \sigma_{e^+e^- Z} &= \frac{2 (\sin^2 \theta_W - \frac{1}{2})^2}{\cos^2 \theta_W} \times v \sigma_{e^+\nu W^-} \Big|_{m_W \rightarrow m_Z} \\ &\simeq 0.19 \times v \sigma_{e^+\nu W^-} \Big|_{m_W \rightarrow m_Z}. \end{aligned} \quad (26)$$

Adding the four contributions to W/Z -strahlung, we find

$$v \sigma_{W/Z\text{-strahlung}} = 2.84 \times v \sigma_{e^+\nu W^-}. \quad (27)$$

IV. DISCUSSION AND CONCLUSIONS

There are clear advantages and disadvantages of seeking photon- versus W/Z -bremsstrahlung as an indirect signature of dark matter. With photon bremsstrahlung, the photon itself is easily detected. Its energy spectrum may then be readily compared to model predictions. With W -strahlung, it is the decay products of the W decay which must be sought. Their spectra are less attributable to the model of dark matter annihilation. However, the total rate for W/Z -strahlung exceeds that of photon-strahlung. Photons couple with strength e , W 's couple with strength $g/\sqrt{2} = e/(\sqrt{2} \sin \theta_W)$, and Z 's couple to neutrinos with strength $g/(2 \cos \theta_W) = e/(2 \cos \theta_W \sin \theta_W)$. Therefore in the high energy limit where the W and Z masses can be neglected, we expect

$$\sigma_{e^+\nu W^-} = \frac{1}{2 \sin^2 \theta_W} \sigma_{e^+e^- \gamma} = 2.17 \sigma_{e^+e^- \gamma}. \quad (28)$$

So, in the high energy limit where $m_\chi \gtrsim 300\text{GeV} \gg m_W$, the total cross section becomes

$$\begin{aligned} \sigma_{\text{brem, total}} &= \sigma_{e^+\nu W^-} + \sigma_{\bar{\nu}e^-W^+} \\ &\quad + \sigma_{\bar{\nu}\nu Z} + \sigma_{e^+e^-Z} + \sigma_{e^+e^-\gamma} \\ &= 7.16 \sigma_{e^+e^-\gamma}. \end{aligned} \quad (29)$$

Furthermore, the varied decay products of the W/Z allow more multi-messenger experiments to engage in the dark matter search. Charged leptons, protons and antiprotons, neutrinos, and even deuterons are expected, at calculable rates and with predictable spectra. Importantly, hadronic decay products are unavoidable, despite a purely leptonic tree-level annihilation. The tens of millions of Z events produced at CERN's e^+e^- collider show in detail what the branching fractions and spectra are for each kind of decay product. We will soon update our Ref. [9] to reveal the favorable prospects for using W -strahlung decay products as indirect signatures for dark matter.

The lifting of the helicity suppression is most significant in the limit where the mass of the boson mediating dark matter annihilation does not greatly exceed the mass of the dark matter particle. This is true both for photon bremsstrahlung and for W/Z -bremsstrahlung. In this limit, we find the three body final state annihilation channels can significantly dominate over two body annihilation channels. The region of parameter space where χ and η are approximately degenerate is of great interest in many models, since it coincides with the co-annihilation region where both $\chi\chi$ and $\chi\eta$ annihilations are important in determining the relic dark matter density at the time of freezeout in the early Universe, often a favored parameter region in SUSY scenarios.

ACKNOWLEDGEMENTS

We thank Paolo Ciafaloni, Alfredo Urbano, and Ray Volkas for helpful discussions. NFB was supported by the Australian Research Council, AJG and TDJ were supported by the Commonwealth of Australia, and TJW was supported in part by U.S. DoE grant DE-FG05-85ER40226.

Appendix A: Class of Models for which $\chi\chi \rightarrow \ell\bar{\ell}$ Annihilation is Suppressed

Consider DM annihilation to a pair of leptons via an s -channel process, for which the matrix elements are product of bilinears of the form $(\bar{\chi} \Gamma_1 \chi)(\bar{\ell} \Gamma_2 \ell)$. By the process of Fierz rearrangement, we can always and easily bring the fermion bilinears in $2 \rightarrow 2$ scattering into this form. To understand which processes are helicity or velocity suppressed, and which are not, we may set v^2 to zero in the χ -current (appropriate for annihilation of non-relativistic DM) and m_ℓ^2 to zero in the lepton current (appropriate for the production of highly relativistic

fermions). The results are given in in Table I of the Appendix. One can read across rows of this table to discover that the only unsuppressed s -channel products of bilinears for the $2 \rightarrow 2$ process are those of the pseudo-scalar, vector, and tensor. For t -channel and u -channel annihilation processes, one may simply use a Fierz transform to convert the amplitudes to s -channel form, and then apply logic similar to that given above. For Majorana dark matter, the vector and tensor bilinears are disallowed by charge-conjugation arguments. The proscription is absolute in the four-Fermi limit where u - and t -channel propagators are identical. More generally, when u and t are not negligible compared to the mass of the exchanged particle, the cancellation between u - and t -channel graphs is incomplete, and the vector and tensor couplings are suppressed but not forbidden.

In Appendix B below we formulate the Fierz transformations first in the standard basis, and then in a chiral basis, the basis most relevant to modern models. See also Ref. [23] for a comprehensive discussion of enhanced/suppressed DM annihilation modes.

Appendix B: Useful Fierz identities

We summarize some useful (and correct) Fierz identities below. An expanded discussion of standard and chiral Fierz transforms may be found in Ref. [1].

As noted in Appendix A and emphasized in [1], the advantage of working with Fierzized amplitudes is that one can immediately see whether the amplitude is velocity-unsuppressed (s -wave) or velocity suppressed (p -wave and higher L). To summarize the meaning of Table 1, a Fierzized s -channel amplitude for $2 \rightarrow 2$ annihilation is neither velocity nor helicity suppressed if the amplitude is pseudoscalar, vector, or tensor. In the class of models we examine, there are no pseudoscalar or tensor amplitudes. The vector amplitude is suppressed by subtraction of a graph and its crossed version. Such subtraction necessarily occurs for Majorana dark matter, since the annihilating particles are identical fermions, and therefore must be crossed (interchanged). The subtraction suppresses the amplitude. If the cancellation is complete, there is no s -channel vector amplitude. If the cancellation is only partial due to non-cancelling pre-factors, then the amplitude is suppressed but nonzero. When the cancellation is partial, the calculation may proceed more easily without Fierzing. Such is the case examined in this work. However, the Fierzing of amplitudes still offer some insight which we wish to exploit in these Appendices.

1. Fierz Transformations in the Standard Basis

The procedure for Fierz transformations in the standard (Dirac) basis of gamma-matrices can be found in, e.g., [24], while Fierz transformations with more general bases of gamma-matrices are laid down in [25]. The start-

s-channel bilinear $\bar{\Psi} \Gamma_D \Psi$		$v = 0$ limit		$M = 0$ limit	
		parallel spinors	antiparallel spinors	parallel spinors	antiparallel spinors
scalar	$\bar{\Psi} \Psi$	0	0	\sqrt{s}	0
pseudo-scalar	$\bar{\Psi} i\gamma_5 \Psi$	$-2iM$	0	$-i\sqrt{s}$	0
axial-vector	$\bar{\Psi} \gamma_5 \gamma^0 \Psi$	$2M$	0	0	0
	$\bar{\Psi} \gamma_5 \gamma^j \Psi$	0	0	0	$\sqrt{s}(\pm\delta_{j1} - i\delta_{j2})$
vector	$\bar{\Psi} \gamma^0 \Psi$	0	0	0	0
	$\bar{\Psi} \gamma^j \Psi$	$\mp 2M \delta_{j3}$	$-2M(\delta_{j1} \mp i\delta_{j2})$	0	$-\sqrt{s}(\delta_{j1} \mp i\delta_{j2})$
tensor	$\bar{\Psi} \sigma^{0j} \Psi$	$\mp 2iM \delta_{j3}$	$-2iM(\delta_{j1} \pm \delta_{j2})$	$-i\sqrt{s} \delta_{j3}$	0
	$\bar{\Psi} \sigma^{jk} \Psi$	0	0	$\pm\sqrt{s} \delta_{j1} \delta_{k2}$	0
pseudo-tensor	$\bar{\Psi} \gamma_5 \sigma^{0j} \Psi$	0	0	$\pm i\sqrt{s} \delta_{j3}$	0
	$\bar{\Psi} \gamma_5 \sigma^{jk} \Psi$	$\mp 2M \delta_{j1} \delta_{k2}$	$-2M(\delta_{j2} \delta_{k3} \mp i\delta_{j3} \delta_{k1})$	$-\sqrt{s} \delta_{j1} \delta_{k2}$	0

TABLE I. Extreme non-relativistic and extreme relativistic limits for s-channel bilinears. In order for a term with an initial-state DM bilinear and a final-state lepton bilinear to remain unsuppressed, the DM bilinear must have a non-zero entry in the appropriate cell of the “ $v = 0$ limit” columns, and the lepton bilinear must have a non-zero term in the appropriate cell of the “ $M = 0$ limit” columns. Otherwise, the term is suppressed. (The tensor and pseudo-tensor are not independent, but rather are related by $\gamma_5 \sigma^{\mu\nu} = \frac{i}{2} \epsilon^{\mu\nu\alpha\beta} \sigma_{\alpha\beta}$.) We recall that antiparallel spinors correspond to parallel particle spins (and antiparallel particle helicities for the $M = 0$ current), and vice versa. Amplitudes are shown for $\bar{u} \Gamma_D v = [\bar{v} \Gamma_D u]^*$. The two-fold \pm ambiguities reflect the two-fold spin assignments for parallel spins, and separately for antiparallel spins. For s-wave annihilation of *Majorana* DM, the χ must have opposite spins to correctly antisymmetrize their wavefunction, and thus only the parallel spinors columns are relevant.

ing point is to define a basis $\{\Gamma^B\}$ and a dual basis $\{\Gamma_B\}$, each spanning 4×4 matrices over the complex number field \mathcal{C} , such that an orthogonality relation holds. The standard Fierz transformation uses the “hermitian” bases

$$\begin{aligned} \{\Gamma^B\} &= \{\mathbb{1}, i\gamma_5, \gamma^\mu, \gamma_5 \gamma^\mu, \sigma^{\mu\nu}\}, \quad \text{and} \\ \{\Gamma_B\} &= \{\mathbb{1}, (-i\gamma_5), \gamma_\mu, (-\gamma_5 \gamma_\mu), \frac{1}{2} \sigma_{\mu\nu}\}, \end{aligned} \quad (\text{B1})$$

respectively. Because of their Lorentz and parity transformation properties, these basis matrices and their duals are often labeled as S and \tilde{S} (scalars), P and \tilde{P} (pseudoscalars), V and \tilde{V} (vectors), A and \tilde{A} (axial vectors), and T and \tilde{T} (antisymmetric tensors).

Using orthogonality and completeness properties, any 4×4 matrices X and Y may be expressed as

$$\begin{aligned} (X)[Y] &= (X\mathbb{1})[\mathbb{1}Y] = \frac{1}{4} (X\Gamma^B Y) [\Gamma_B] \\ &= \frac{1}{4^2} \text{Tr}[X\Gamma^B Y\Gamma_C] (\Gamma^C) [\Gamma_B], \end{aligned} \quad (\text{B2})$$

where we have adopted Takahashi’s notation [26] where matrix indices are replaced by parentheses (\dots) and brackets $[\dots]$, in an obvious way. Alternatively, we may express any 4×4 matrices X and Y as

$$\begin{aligned} (X)[Y] &= (X\mathbb{1})[Y\mathbb{1}] = \frac{1}{4} (X\Gamma^B) [Y\Gamma_B] \\ &= \frac{1}{4^3} \text{Tr}[X\Gamma^B \Gamma_C] \text{Tr}[Y\Gamma_B \Gamma^D] (\Gamma^C) [\Gamma_D]. \end{aligned} \quad (\text{B3})$$

The RHS’s of Eqs. (B2) and (B3) offer two useful options for Fierzing matrices.

To give the common example, for 2 fermions $\rightarrow 2$ fermions processes, the vertex matrices are of Dirac type, $X = \Gamma^D$ and $Y = \Gamma_D$. the result from Eq. (B2) is then a 5×5 matrix of numbers which linearly relate the t - and u -channel bilinears to a sum over s -channel Dirac bilinears (see Ref. [1] or most QFT textbooks for details). However, for the $2 \rightarrow 3$ processes such as the W -bremsstrahlung which we consider herein, the matrices X and Y are not simple Dirac matrices. For this more general case, the full power of Eq. (B2) comes into play, as we shall see.

At this point, we call attention to the first expression in Eq. (B2),

$$(X)[Y] = \frac{1}{4} (X\Gamma^B Y) [\Gamma_B]. \quad (\text{B4})$$

In the notation of the textbook by Okun [27], this identity should read

$$F_l^i G_k^m = \frac{1}{4} \sum_A \Delta_A (F\gamma_A G)_l^m (\gamma_A)_k^i, \quad (\text{B5})$$

but does not. In the published expression of Ref. [27] the indices are incorrectly interchanged, equivalent to exchanging F and G on one side of the equation. It was the use of the incorrect expression in [27] that led to an incorrect calculation of the cross section in [1].

2. Fierz Transformations in the Chiral Basis

Helicity projection operators are essential in chiral gauge theories, so it is worth considering the reformu-

lation of Fierz transformations in the chiral basis [25]. We place hats above the generalized Dirac matrices constituting the chiral basis. These matrices are

$$\begin{aligned} \{\hat{\Gamma}^B\} &= \{P_R, P_L, P_R\gamma^\mu, P_L\gamma^\mu, \frac{1}{2}\sigma^{\mu\nu}\}, \quad \text{and} \\ \{\hat{\Gamma}^B\} &= \{P_R, P_L, P_L\gamma_\mu, P_R\gamma_\mu, \frac{1}{2}\sigma_{\mu\nu}\}. \end{aligned} \quad (\text{B6})$$

Using completeness of the basis, one arrives at a master formula which expands the outer product of two chiral matrices in terms of their Fierz forms:

$$(\hat{\Gamma}^D) [\hat{\Gamma}^E] = \frac{1}{4} \text{Tr} [\hat{\Gamma}^D \hat{\Gamma}^C \hat{\Gamma}^E \hat{\Gamma}^B] (\hat{\Gamma}^B) [\hat{\Gamma}^C], \quad (\text{B7})$$

Evaluating the trace in Eq. B7 leads to the Fierz transformation matrix in the chiral-basis, presented in [1]) and repeated here:

$$\begin{pmatrix} (P_R) [P_R] \\ (P_L) [P_L] \\ (\hat{T}) [\hat{T}] \\ (\gamma_5 \hat{T}) [\hat{T}] \\ (P_R) [P_L] \\ (P_R\gamma^\mu) [P_L\gamma_\mu] \\ (P_L) [P_R] \\ (P_L\gamma^\mu) [P_R\gamma_\mu] \\ (P_R\gamma^\mu) [P_R\gamma_\mu] \\ (P_L\gamma^\mu) [P_L\gamma_\mu] \end{pmatrix} = \frac{1}{4} \begin{pmatrix} 2 & 0 & 1 & 1 & & & & & & & \\ 0 & 2 & 1 & -1 & & & & & & & \\ 6 & 6 & -2 & 0 & & & & & & & \\ 6 & -6 & 0 & 2 & & & & & & & \\ & & & & 0 & 2 & & & & & \\ & & & & 8 & 0 & & & & & \\ & & & & & & 0 & 2 & & & \\ & & & & & & 8 & 0 & & & \\ & & & & & & & & -4 & 0 & \\ & & & & & & & & 0 & -4 & \end{pmatrix} \begin{pmatrix} (P_R) [P_R] \\ (P_L) [P_L] \\ (\hat{T}) [\hat{T}] \\ (\gamma_5 \hat{T}) [\hat{T}] \\ (P_R) [P_L] \\ (P_R\gamma^\mu) [P_L\gamma_\mu] \\ (P_L) [P_R] \\ (P_L\gamma^\mu) [P_R\gamma_\mu] \\ (P_R\gamma^\mu) [P_R\gamma_\mu] \\ (P_L\gamma^\mu) [P_L\gamma_\mu] \end{pmatrix}. \quad (\text{B8})$$

Non-explicit matrix elements in (B8) are zero, and we have introduced a shorthand \hat{T} for either $\hat{\Gamma}^T = \frac{1}{2}\sigma^{\mu\nu}$ or $\hat{\Gamma}^T = \frac{1}{2}\sigma_{\mu\nu}$. In Eq. (B8) we have included one non-member of the basis set, namely $\gamma_5 \hat{T}$; it is connected to \hat{T} via the relation $\gamma_5 \sigma^{\mu\nu} = \frac{i}{2}\epsilon^{\mu\nu\alpha\beta}\sigma_{\alpha\beta}$.

Of particular relevance to the class of models we examine, is that $(P_R) [P_L]$ Fierz to $\frac{1}{4}(P_R\gamma^\mu) [P_L\gamma_\mu]$, and similar for $R \leftrightarrow L$. Thus, the P_R and P_L couplings of the u - and t -channel scalars Fierz to vector and axial vector couplings in the s -channel. The vector coupling's are suppressed by the Majorana condition, and the axial vector couplings are suppressed by the $L = 0$ nature of the axial three-vector.

Appendix C: Fierz transformed matrix elements

Upon applying Eq. (B4) to Fierz transform the matrix elements of Eqn.(4)–(9) we find

$$\begin{aligned} \mathcal{M}_a &= \frac{igf^2}{\sqrt{2}q_1^2} \frac{1}{t_1 - m_\eta^2} \frac{1}{2} \left(\bar{v}(k_2)\gamma_\alpha P_R u(k_1) \right) \\ &\quad \times \left(\bar{u}(p_1)\gamma^\mu \not{q}_1 \gamma^\alpha P_L v(p_2) \right) \epsilon_\mu^Q, \end{aligned} \quad (\text{C1})$$

$$\begin{aligned} \mathcal{M}_b &= \frac{igf^2}{\sqrt{2}q_1^2} \frac{1}{u_1 - m_\eta^2} \frac{1}{2} \left(\bar{v}(k_2)\gamma_\alpha P_L u(k_1) \right) \\ &\quad \times \left(\bar{u}(p_1)\gamma^\mu \not{q}_1 \gamma^\alpha P_L v(p_2) \right) \epsilon_\mu^Q, \end{aligned} \quad (\text{C2})$$

$$\begin{aligned} \mathcal{M}_c &= \frac{-igf^2}{\sqrt{2}q_2^2} \frac{1}{t_2 - m_\eta^2} \frac{1}{2} \left(\bar{v}(k_2)\gamma_\alpha P_R u(k_1) \right) \\ &\quad \times \left(\bar{u}(p_1)\gamma^\alpha \not{q}_2 \gamma^\mu P_L v(p_2) \right) \epsilon_\mu^Q, \end{aligned} \quad (\text{C3})$$

$$\begin{aligned} \mathcal{M}_d &= \frac{-igf^2}{\sqrt{2}q_2^2} \frac{1}{u_2 - m_\eta^2} \frac{1}{2} \left(\bar{v}(k_2)\gamma_\alpha P_L u(k_1) \right) \\ &\quad \times \left(\bar{u}(p_1)\gamma^\alpha \not{q}_2 \gamma^\mu P_L v(p_2) \right) \epsilon_\mu^Q, \end{aligned} \quad (\text{C4})$$

$$\begin{aligned} \mathcal{M}_e &= \frac{-igf^2}{2\sqrt{2}} \frac{(2k_1 - 2p_1 - Q)^\mu}{(t_3' - m_\eta^2)(t_3 - m_\eta^2)} \left(\bar{v}(k_2)\gamma_\alpha P_R u(k_1) \right) \\ &\quad \times \left(\bar{u}(p_1)\gamma^\alpha P_L v(p_2) \right) \epsilon_\mu^Q, \end{aligned} \quad (\text{C5})$$

$$\begin{aligned} \mathcal{M}_f &= \frac{-igf^2}{2\sqrt{2}} \frac{(2k_2 - 2p_1 - Q)^\mu}{(u_3' - m_\eta^2)(u_3 - m_\eta^2)} \left(\bar{v}(k_2)\gamma_\alpha P_L u(k_1) \right) \\ &\quad \times \left(\bar{u}(p_1)\gamma^\alpha P_L v(p_2) \right) \epsilon_\mu^Q. \end{aligned} \quad (\text{C6})$$

The Fierz transformed matrix elements of Eq.(C1-C6) correct those given in Ref. [1] (which are in error due to the use of an incorrect Fierz identity from Ref. [27]).

Alternatively, we may apply Eq.(B7) to transform Eqs.(4)-(9). After a bit of algebra we get a pleasant factorized form for the bilinear currents. We show details for the first one, and then summarize the results for current products of the other matrix elements.

The current product in amplitude M_a of Eq.(4) is

$$\left(\bar{v}(k_2)P_L v(p_2) \right) \left(\bar{u}(p_1)\not{\epsilon}^Q P_L \not{q}_1 u(k_1) \right). \quad (\text{C7})$$

We write this current product in Takahashi notation and

then use Eq.(B7) to get

$$\begin{aligned} [P_L](\not{\epsilon}^Q P_L \not{q}_1) &= \frac{1}{4} \text{Tr}[P_L \Gamma^C \not{\epsilon}^Q P_L \not{q}_1 \Gamma_B] (\Gamma^B) (\Gamma^C) \\ &= \frac{1}{4} \text{Tr}[P_L \gamma^\alpha \not{\epsilon}^Q P_L \not{q}_1 \gamma_\beta (P_R \gamma^\beta) [P_L \gamma_\alpha]. \end{aligned} \quad (\text{C8})$$

In going from the first equality to the second, we insert the only values for Γ^C and Γ_B allowed by the helicity projectors in the string of gamma matrices. Finally, we may invert the sequence in the trace, and remove the Takahashi notation to write the result as

$$\frac{1}{4} \text{Tr}[P_R \not{\epsilon}^Q P_L \not{q}_1 \gamma_\beta \gamma^\alpha] \times (\bar{u}(p_1) P_R \gamma^\beta v(p_2)) (\bar{v}(k_2) P_L \gamma_\alpha u(k_1)). \quad (\text{C9})$$

Amplitude M_b is computed in a similar way. In addition, it is useful to use the identity for a Majorana current

$$(\bar{v}(k_1) P_L \gamma_\alpha u(k_2)) = (\bar{v}(k_2) P_R \gamma_\alpha u(k_1)) \quad [\text{Majorana}] \quad (\text{C10})$$

to put the final result in a form similar to that for amplitude M_a .

The other current products are reduced in a similar fashion. The final result for the product of currents after Fierzing is

$$\begin{aligned} &\frac{1}{4} (\bar{v}(k_2) P \gamma^\alpha u(k_1)) (\bar{u}(p_1) P_R \gamma^\beta v(p_2)) \quad (\text{C11}) \\ &\times \begin{cases} \text{Tr}[P_R \not{\epsilon}^Q \not{q}_1 \gamma_\beta \gamma_\alpha], & \text{for } M_a, M_b \\ \text{Tr}[P_L \not{\epsilon}^Q \not{q}_2 \gamma_\beta \gamma_\alpha], & \text{for } M_c, M_d \\ 2g_{\alpha\beta}, & \text{for } M_e, M_f. \end{cases} \end{aligned}$$

In addition, the unspecified projector P in the first common factor is P_L for amplitudes M_a , M_c , M_e , and P_R

for the amplitudes M_b , M_d , M_f derived from the crossed graphs.

What can we learn from this exercise? For graphs M_e and M_f the Fierzed currents are the same as in the $2 \rightarrow 2$ case. This fact is not surprising since in these graphs the internal W emission does not perturb the form of the currents and their product. However, for the other four graphs with W emission occurring on a fermion leg, the form of the current product is quite different from the $2 \rightarrow 2$ case. With $2 \rightarrow 3$ scattering, the Lorentz index of each current need not contract directly with the other. Referring to Table 1, one sees that unsuppressed Majorana annihilation amplitudes become possible for the axial vector combination $(\gamma_5 \gamma^0) [\gamma_5 \vec{\gamma}_T]$, and for the vector combination $(\gamma^3) [\vec{\gamma}_T]$, providing the trace post-factors in Eq. (C11) do not vanish. These combinations are at the heart of the unsuppression which we have presented in this paper.

Also, for $m_\eta^2 \gg t, u$, the non-current factors in amplitudes M_a and M_b are the same, as are the non-current factors in amplitudes M_c and M_d . Then the subtraction of one from the other leads to a pure axial vector coupling in the Majorana current. This in turn leads to an effectively pure axial vector coupling in the final state lepton current. This effective axial vector-axial vector coupling of currents was advertised earlier. However, for values of t and u which are non-negligible when compared to m_η^2 , there is some residual vector coupling. In this more complicated case, it is probably best to directly calculate rates without Fierzing the currents. Such is the course followed in the main text of this paper.

-
- [1] N. F. Bell, J. B. Dent, T. D. Jacques, T. J. Weiler, Phys. Rev. **D83**, 013001 (2011) [arXiv:1009.2584 [hep-ph]].
- [2] V. Berezhinsky, M. Kachelriess and S. Ostapchenko, Phys. Rev. Lett. **89**, 171802 (2002) [arXiv:hep-ph/0205218].
- [3] M. Kachelriess and P. D. Serpico, Phys. Rev. D **76**, 063516 (2007) [arXiv:0707.0209 [hep-ph]].
- [4] N. F. Bell, J. B. Dent, T. D. Jacques and T. J. Weiler, Phys. Rev. D **78**, 083540 (2008) [arXiv:0805.3423].
- [5] J. B. Dent, R. J. Scherrer and T. J. Weiler, Phys. Rev. D **78**, 063509 (2008) [arXiv:0806.0370 [astro-ph]].
- [6] M. Kachelriess, P. D. Serpico, M. A. Solberg, Phys. Rev. **D80**, 123533 (2009) [arXiv:0911.0001 [hep-ph]].
- [7] P. Ciafaloni, A. Urbano, Phys. Rev. **D82**, 043512 (2010) [arXiv:1001.3950 [hep-ph]].
- [8] P. Ciafaloni, D. Comelli, A. Riotto, F. Sala, A. Strumia, A. Urbano, JCAP **1103**, 019 (2011) [arXiv:1009.0224 [hep-ph]].
- [9] N. F. Bell, J. B. Dent, T. D. Jacques, T. J. Weiler, [arXiv:1101.3357 [hep-ph]].
- [10] Massive three body final states were considered in X. L. Chen and M. Kamionkowski, JHEP **9807**, 001 (1998).
- [11] L. Bergstrom, Phys. Lett. B **225**, 372 (1989).
- [12] R. Flores, K. A. Olive and S. Rudaz, Phys. Lett. B **232**, 377 (1989).
- [13] E. A. Baltz and L. Bergstrom, Phys. Rev. D **67**, 043516 (2003) [arXiv:hep-ph/0211325].
- [14] T. Bringmann, L. Bergstrom and J. Edsjo, JHEP **0801**, 049 (2008) [arXiv:0710.3169 [hep-ph]].
- [15] L. Bergstrom, T. Bringmann and J. Edsjo, Phys. Rev. D **78**, 103520 (2008) [arXiv:0808.3725 [astro-ph]].
- [16] V. Barger, Y. Gao, W. Y. Keung and D. Marfatia, Phys. Rev. D **80**, 063537 (2009) [arXiv:0906.3009 [hep-ph]].
- [17] Q. H. Cao, E. Ma and G. Shaughnessy, Phys. Lett. B **673**, 152 (2009) [arXiv:0901.1334 [hep-ph]].
- [18] E. Ma, Phys. Rev. Lett. **86**, 2502 (2001) [arXiv:hep-ph/0011121].
- [19] H. Goldberg, Phys. Rev. Lett. **50**, 1419 (1983), making use of some earlier Fierzing by P. Fayet, Phys. Lett. B **86**, 272 (1979). See L. M. Krauss, Nucl. Phys. **B227**, 556 (1983) for cosmological implications.
- [20] H. E. Haber and G. L. Kane, Phys. Rept. **117**, 75 (1985), see Fig.72b on p. 221 of appendix C.

- [21] L.D. Landau and E.M. Lifschitz, “The Classical Theory of Fields”, Pergamon Press, 4th revised English edition, pages 32-34.
- [22] P. Gondolo and G. Gelmini, Nucl. Phys. B360, 145 (1991).
- [23] M. Lindner, A. Merle and V. Niro, arXiv:1005.3116 [hep-ph].
- [24] C. Itzykson and J.B. Zuber, Quantum Field Theory, pages 161-2, Dover Pr., 1980.
- [25] C. C. Nishi, Am. J. Phys. **73**, 1160 (2005) [arXiv:hep-ph/0412245].
- [26] Y. Takahashi, “The Fierz Identities”, in *Progress in Quantum Field Theory*, ed. H. Ezawa and S. Kamefuchi (North Holland, Amsterdam, 1986), p. 121.
- [27] L. B. Okun, *Leptons And Quarks*, Amsterdam, Netherlands, North-Holland (1982) 361p, section 29.3.5.